35. 周期的境界条件下における核物質の熱的性質

Thermal properties of nuclear matter under the periodic boundary condition

Naohiko Otuka * and Akira Ohnishi
Division of Physics, Graduate School of Science, Hokkaido University, Sapporo 060-0810, JAPAN
(June 18, 1999)

We present the thermal properties of nuclear matter under the periodic boundary condition by the use of our hadronic nucleus-nucleus cascade model (HANDEL) which is developed to treat relativistic heavy-ion collisions from BNL-AGS to CERN-SPS. We first show some results of $p-p$ scattering calculation in our new version which is improved in order to treat isospin ratio and multiplicity more accurately. We then display the results of calculation of nuclear matter with baryon density $\rho_b = 0.77$ fm^3 at some energy densities. Time evolution of particle abundance and temperature are shown.

I. INTRODUCTION

The main aim of relativistic heavy ion collision study is acquiring the knowledge of the equation of state of nuclear matter under extreme conditions. Experimentally the temperatures and chemical potentials at the freeze-out are discussed based on the data at BNL-AGS [1] and CERN-SPS [2]. When we study thermodynamical character of nuclear matter from heavy ion collisions, it is important whether the matter formed during collision reaches equilibrium or not. The fact that the transverse momentum distributions of proton and pion from the experiment are to be well fitted with the Boltzmann distribution with flow effects shows that the matter approximately reaches thermal equilibrium at the freeze-out. Transverse momentum distributions are studied also by using microscopic transport calculations such as JAM [3], RBUU [4], RQMD [5], UrQMD [6], ARC [7], ART [8] at AGS energies. They can reproduce transverse spectra, although these models has different assumptions for particle production from each other.

In RQMD and UrQMD baryon-baryon inelastic scattering can produce baryonic resonances whose masses are below 2GeV, then many particles are produced through the decay of baryonic resonances such as $R_1 \rightarrow m_1 + R_2 + \ldots$, $R_2 \rightarrow \ldots$, where R_i and m_i denote a baryonic resonance and a meson, respectively. In addition to these processes, particles are also produced through string decays when the invariant mass of two incidental nucleons is much larger than the 1-pion production threshold. Meanwhile only several low-lying baryonic resonances are included in ARC and ART. In these models, multi-particle production are realized through direct particle production as $N_1 + N_2 \rightarrow B_1 + B_2 + m_1 + m_2 \ldots$, where N_i and B_i denote a nucleon and a baryon, respectively. The detailed balance is usually violated in treating string decays and direct particle production because inverse processes are not taken into account. This point is important when we discuss the statistical property of nuclear matter using microscopic transport calculation.

In this report we discuss the statistical property of nuclear matter by the use of hadronic nucleus-nucleus cascade model (HANDEL) which is developed for the calculation of relativistic heavy-ion collisions from BNL-AGS to CERN-SPS energies and includes multi-particle production. First we introduce our model and then we show the results of calculation of nuclear matter under periodic boundary conditions.

II. MODEL

In our previous model (referred to as Model-B in [9]), particle production is realized through

(1) decay of baryonic resonances $\Delta(1232)$, $N^*(1440)$ and $N^*(1535)$ which are generated by

$$NN \leftrightarrow NR,\ \Delta\Delta,\ \Delta N^*(1440), \tag{1}$$

where R denotes $\Delta(1232)$, $N^*(1440)$ or $N^*(1535)$, and

(2) direct particle production,

$$NN \rightarrow NN\rho,\ NN\omega,\ \Delta\Delta\pi, \tag{2}$$

$$NN \rightarrow \Delta\Delta\rho,\ N^*(1440)\Delta\omega. \tag{3}$$

The maximum number of pions from nucleon-nucleon collision is three in the resonance model (via $NN \rightarrow \Delta(1232)N(1440)$) and six in the direct production(via $NN \rightarrow \Delta(1232)N(1440)\omega$). This description of particle production which is an extension of the model used in

*e-mail: ohtsuka@nucl.sci.hokudai.ac.jp

ART can reproduce the average multiplicity of charged pions in $p-p$ collision (experimental value is 3.43 [12]). However this previous model has some defects. First, direct particle production violates the detailed valance because our model does not contain multi-particle collision processes. Secondly this model may reveal incorrect property for isospin thermalization due to the large omega production rate. The omega production is introduced somewhat artificially to earn the pion yield and to carry a large part of multi-particle production channels at high energies. However some particle production, for example $pp \to pp\pi^+\pi^+\pi^+\pi^-\pi^-\pi^-$, cannot be treated by the latter process in the reactions of Eq.(3) because the final state of this process must contain at least one π^0. Thirdly the particle yield is insufficient at more energetic collisions than AGS energy.

To improve these points we incorporate new framework of particle production into the current model. In this new model we use the same cross sections as previous ones for the channel which contain less than 4 pions in exit channel (corresponding to the channels in Eqs.(1) and (2)).

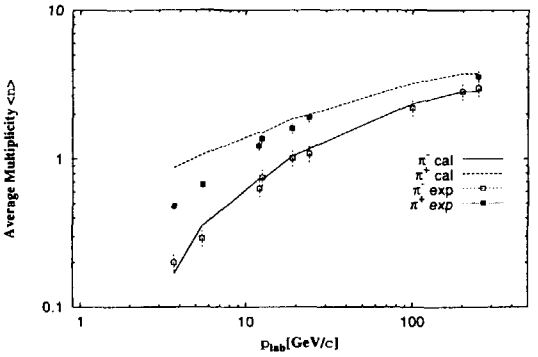

FIG. 1. Average multiplicity of charged pions in $p-p$ inelastic scattering calculated in our model for π^-(solid) and π^+(dashed). Experimental data for π^-(open squares with dashed error bars) and π^+(solid squares with dotted error bars) are taken from Ref. [13].

The remainder of cross section is distributed to multi-pion production

$$NN \to NN\pi\pi\pi\pi, NN \to NN\pi\pi\pi\pi\pi, ... \qquad (4)$$

We set an upper limit of pion number in the exit channel to 20. The ratio of cross sections for each multiplicity to total remainder is determined from the result of JAM which is the transport model based on HIJING [10] and PYTHIA [11] and also includes hadron-hadron scattering in order to treat final state interactions of hadronic gas. As presented in Fig. 1 our new model yields suitable number of charged pions both at BNL-AGS energies ($\sim$ 10GeV/c) and at CERN-SPS energies($\sim$ 200GeV/c). The calculated inelastic cross sections for several channels which are shown in Fig. 2 by solid points are also in good agreement with experimental data.

When we calculate heavy ion collisions or nuclear matter, we also include baryon-meson inelastic scattering ,

$$\pi N \leftrightarrow \Delta(1232),\ N^*(1440),\ N^*(1535), \qquad (5)$$

$$\eta N \to N^*(1535), \qquad (6)$$

$$\pi N \leftrightarrow KY, K^*Y, \qquad (7)$$

and meson-meson inelastic scattering:

$$\pi\pi \leftrightarrow \rho \qquad (8)$$

as elementary processes in our model, where $K = (K^0, K^+)$ and $Y = (\Lambda, \Sigma)$.

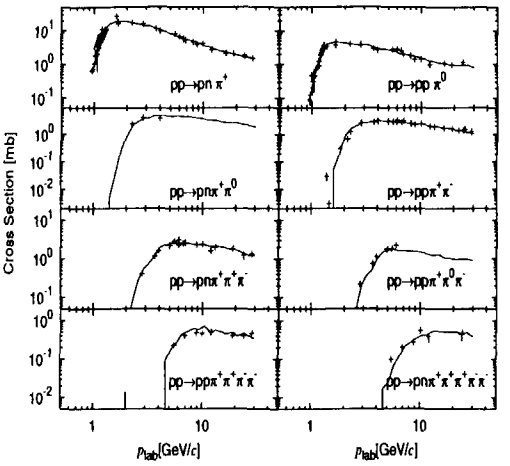

FIG. 2. Inelastic cross sections of $p-p$ collision. The solid lines denote the results of our calculation, while crosses denote experimental data taken from Ref. [14]

III. RESULTS OF CALCULATIONS UNDER PERIODIC BOUNDARY CONDITION

In the present work, we have made simulation calculation of nuclear matter at 4 different energies (e=1,17, 1.56, 1.87, 2.24 GeV/fm^3). The box is 8-fm cube, and contains 158 protons and 236 neutrons (baryon density ρ_b=0.77/fm^3). The isospin ratios and energy densities correspond to those of collision system of Au+Au at incidental projectile momenta p_{lab}=4.0, 8.0, 12.0, 18.0 A GeV/c.

A. Direct particle production and detailed balance

As mentioned in the previous section our current model improves multiplicity and isospin ratio of pion at high

energies, while the violation of detailed valance still remains due to the existence of direct multi-particle production. In order to estimate the effects of this violation, we check the time evolution of collision number ratio between binary collision shown in Eq.(1) and direct particle production shown in Eqs. (2) and (4).

In Fig.3, we show the collision number ratio of multi-particle production to binary collision in $p-p$ inelastic scattering. The relative numbers of multi-particle production are prominent for more energetic gas and at earlier stage ($t \leq 5$ fm/c) and diminish with time evolution. However they do not disappear after the elapse of several tens of fm/c. This means that the inverse processes of multi-particle scattering should not be neglected even after relaxation.

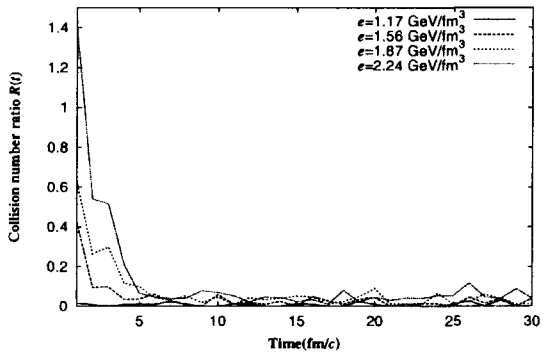

FIG. 3. Collision number ratio of multi-particle production to binary collision in $p-p$ inelastic scattering in nuclear matter with baryon density $\rho_b = 0.77/\mathrm{fm}^3$. Energy densities are e =1.17GeV/fm^3(solid line), 1.56GeV/fm^3(long dashed line). 1.87GeV/fm^3(short dashed line) and 2.24GeV/fm^3(dotted line).

The importance of detailed balance can be understood in another way. Our model includes hyperon production process from πN scattering, $\pi N \rightarrow KY$. To keep detailed balance the inverse process of the above scattering $KY \rightarrow \pi N$ should be also included.

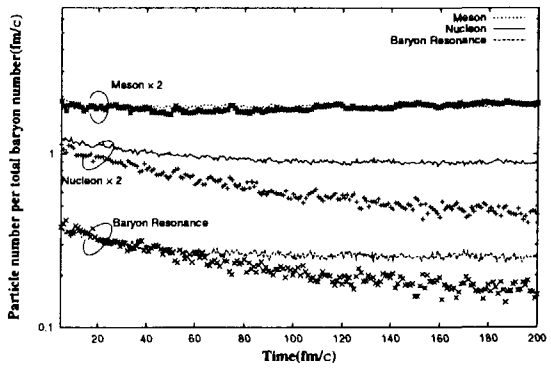

FIG. 4. Time evolution of particle abundance of meson(dotted line), nucleon(solid line) and baryonic resonance(dashed line) with $KY \rightarrow \pi N$ process in nuclear matter at baryon density ρ_b=0.77/fm^3, and the energy density is e=1.87GeV/fm^3. Asterisks, pluses and crosses are the results without $KY \rightarrow \pi N$, respectively. Factor 2 is multiplied to the results of meson and nucleon.

The particle abundance of meson, nucleon and baryonic resonance given in the calculations with and without strangeness pair annihilation (the inverse process in Eq.(7) are displayed in Fig.4.

The sum of nucleon and baryonic resonance (these do not include hyperons) decrease monotonically when we do not take account of the inverse process shown in Eq.(7). The role of this inverse process on chemical equilibration is clearly seen in this figure, even if the process is rare.

B. Relaxation to Thermal and Chemical equilibrium

We discuss temperature and particle abundance at relaxation.

First relaxations of temperature are shown in Fig.5 by symbols. In this calculation temperature is defined as the ratio of pressure to the number density of hadrons,

$$T = \frac{P}{\rho_h} = \frac{T_{xx}+T_{yy}}{2V}\frac{1}{\rho_h} = \frac{1}{2V\rho_h}\sum_{i=1}^{N_h}\frac{p_{xi}^2+p_{yi}^2}{E_i}, \qquad (9)$$

where the summation is taken for all hadrons in a box. N_h and V are the number of hadrons in a box and the volume of the box, respectively, while the pressure P is determined from an average of diagonal component of energy-momentum tensor T_{xx} and T_{yy} per unit volume.

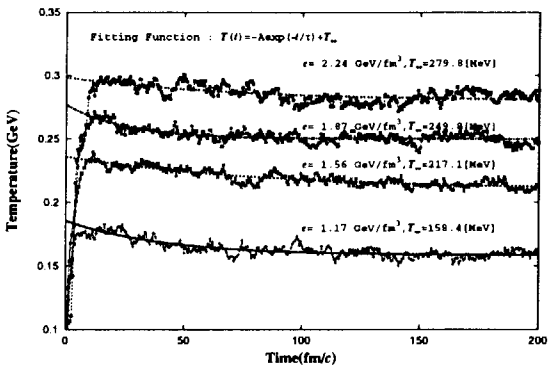

FIG. 5. Time evolution of temperature in nuclear matter with baryon density ρ_b=0.77/fm^3. Energy densities are e=1.17(pluses), 1.56(crosses), 1.87(asterisks) and 2.24(open squares) GeV/fm^3), respectively. Lines are results of fitting to single exponential functions.

As one can see, these temperatures visibly fluctuate around certain temperatures even in the late stage. We

extrapolate a temperature T_∞ by fitting the time dependence of the temperature to a single exponential function. We show temperature at relaxation T_∞ in Fig.6 as a function of energy density.

The results of transport calculation give too high temperatures to meet statistical calculations at the same energy densities. This caloric curve exhibits a striking contrast to the result of URASiMA [15] in which temperature is lower than that in a statistical model at a given energy density and increasing of temperature is strongly suppressed at some temperature around 100 MeV (taking account of pion only).

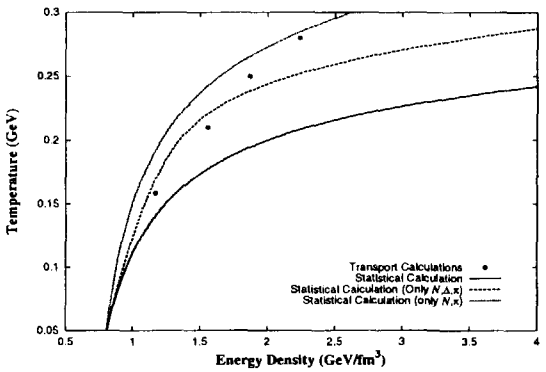

FIG. 6. Caloric curve for nuclear matter. Dotted points are the results of transport calculation, while lines denote the results of statistical calculation for gases with several sets of component. Baryon density is ρ_b=0.77/fm^3.

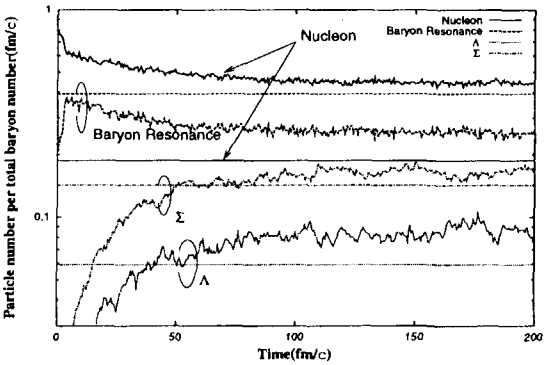

FIG. 7. Time evolution of particle abundance of nucleon(solid line), baryonic resonance(dashed line), Λ(dotted line) and Σ(dashed-dotted line) at ρ_b = 0.77 GeV/fm^3 and e=1.87GeV/fm^3. Straight lines show the results of a statistical model.

In Fig.7 we display the time evolution of particle abundance. Horizontal straight lines represent the results of a statistical model which takes account Fermi-Dirac statics for fermions and Bose-Einstein statics for bosons as well as the baryon number and strangeness conservation. However, we neglected the effects of residual interactions, such as exclusive volume effects, and finite life-times of resonance particles in this statistical treatment.

Abundances of Λ and Σ from our calculation show a reasonable agreement with the statistical model. For the particle abundance of nucleons and baryonic resonances, however, there is a large discrepancy between the results in our calculation and the statistical model. Statistical model predicts that the number of baryonic resonance is superior to that of normal nucleon, while this relation is reversed in our calculation.

IV. DISCUSSION AND OUTLOOK

Here we discuss probable reasons for the discrepancy from the results of transport calculation to that of the statistical model in the particle ratio (Fig.7) and temperature (Fig.5). Using our model, in the earlier stage many mesons are produced through direct particle production which have larger cross sections at higher energies. If we include the inverse processes of direct particle production in the reactions shown in Eqs.(2) and (4), non-excited but *energetic* nucleon pair is produced in many-body scattering such as $B_1B_2m_1m_2.. \rightarrow NN$. In a later stage, hence, more baryonic resonance production remain than in a current treatment and may cause to reverse the particle abundance of nucleons and baryonic resonances. If we take account this point, our current calculation should estimate lower kinetic energy and the temperature than those in the statistical model.

Once we stand for this consideration, however, the caloric curve shown in Fig.6 is incomprehensible. In order to understand these results consistently, we have to study (1) the transport calculation at lower densities where statistical mechanics without residual interactions is expected to give a more reliable value, (2) comparison between the results in the statistical model and in the transport calculation which includes only binary scattering in nucleon-nucleon scattering so that one can keep detailed balance strictly, and (3) the effects of a width of unstable particles on the statistical property in statistical calculations.

[1] L. Ahle *et al.*(E802 Collaboration), Phys. Rev. **C59**, 2173 (1999).
[2] H. Appelshäuser *et al.*(NA49 Collaboration), Phys. Rev. Lett. **82**, 2471 (1999).
[3] Y. Nara, in this proceedings.
[4] P. K. Sahu and A. Ohnishi, in this proceedings.
[5] H. Sorge, H. Stöker and W. Greiner, Ann. Phys.(N.Y.) **192**, 286 (1989).
[6] A. Dumitru, M. Bleicher, S. A. Bass, C. Spieles, L. Neise, H. Stöker and W. Greiner, Phys. Rev. **C57**, 6 (1998).
[7] Y. Pang, T. J. Schlagel and S. H. Kahana, Phys. Rev. Lett. **68**, 2743 (1992).
[8] B. A. Li and C. M. Ko, Phys. Rev. **C52**, 2037 (1995).

[9] Y. Nara, N. Otuka, A. Ohnishi and T. Maruyama, Prog. Theor. Phys. Suppl. **129**, 33 (1997).
[10] X. N. Wang, Phys. Rep. **280**, 287 (1997), X. N. Wang and M. Gyulassy, Comp. Phys. Comm. **83**, 307 (1994).
[11] T. Sjöstrand, Comp. Phys. Comm. **82**, 74 (1994).
[12] V. Blobel *et al.*, Nucl. Phys. **B69**, 454 (1974).
[13] M. Antiunucci, A. Bertin, P. Capiluppi, M. D'Agostino-Bruno, A. M. Rossi, G. Vannini, G. Giacomelli and A. Bussiére. Lett. Nuov. Cim. **6**, 121 (1973).
[14] *Total Cross-sections for the Reactions of High Energy Particles*, edited by A. Baldini, V. Flaminio, W. G. Moorhead and D. R. O. Morrison, (Springer-Verlag, Berlin, 1988).
[15] N. Sasaki and O. Miyamura, Prog. Theor. Phys. Suppl. **129**, 39 (1997).